JOURNAL OF MATERIALS SCIENCE **34** (1999) 1953–1958

# An investigation of the age hardening behavior of PM 2024Al-Fe-Ni alloys and the effect of consolidation conditions

S. XIANG
*Graduate School of Toyama University, Gofuku 3190 Toyama, Japan 930-8555*

K. MATSUKI, N. TAKATSUJI
*Department of Mechanical System Engineering, Faculty of Engineering, Toyama University, Toyama, Japan 930-8555*

T. YOKOTE, J. KUSUI, K. YOKOE
*Toyo Aluminum K. K., Yao, Osaka, Japan 581*

The aging ability of two PM alloys based on 2024Al with Fe and Ni addition has been investigated by means of EDX, XRD, DSC, TEM and Vickers hardness analysis, and compared with that of the base alloy PM 2024 aluminum. Effect of consolidation temperature and powder size on the aging behavior of the 3F5N alloy was also studied. The results showed that the 3F0N alloy, PM 2024Al with 3 mass% Fe single addition, exhibited poor aging ability compared to 2024 alloy. In this alloy, the amount of solid solution Cu was found to decrease by forming $Al_7Cu_2Fe$ compound during solidification, resulting in a lower amount of Cu dissolved into the $\alpha$-Al matrix of the extrusions during the solution treatment. Whereas the 3F5N alloy, PM 2024Al with a 3 mass% Fe and 5 mass% Ni combined addition, showed almost the same age hardenability compared to PM 2024 alloy. Due to the addition of Ni, the amount of insoluble compound $Al_7Cu_2Fe$ was decreased by the formation of $Al_9FeNi$ phase in the 3F5N alloy. Thus, more Cu could be dissolved into the matrix during the solution treatment. A quantity of GPB zone could be formed in the 3F5N alloy during the aging resulting in higher age hardenability than the 3F0N alloy. The extrusion temperature and powder size were found to affect the aging hardenability of the 3F5N extrusions. Although higher age hardenability could be obtained in the 3F5N specimen extruded from powders with the relatively larger diameter, it was found that with decreasing extrusion temperature the higher aging ability could also be obtained in the 3F5N alloy extruded from finer powders. 

## 1. Introduction

With developing application of the Powder Metallurgy (PM) technique, there is one trying to add transition elements into the high strength, heat-treatable 2000 or 7000 series aluminum alloys [1–3]. The aim of this trying is an improvement of the strength at elevated temperature as well as room temperature by combining the effects of both fine dispersoid dispersion strengthening and age hardening. This Rapid Solidification (RS) technique is considered to be one of useful and advanced methods, which is applicable to the other age hardenable aluminum alloys.

However, in the case of PM 2000 series aluminum alloys, one problem has been pointed out [1]. The formation of dispersoids consisting of both the transition elements and the elementary elements, such as Cu and Mg [1], could decrease the concentration of Cu or Mg in solid solution, resulting in poor age hardenability. Concerning this problem, Wilson and Forsyth [4] proved that the combined addition of 1% Ni and 1% Fe to Ingot Metallurgy (IM) Al-2.5%Cu-1.2%Mg alloy was effective to prevent the decrease of age hardenability. However, for developing an elevated temperature aluminum alloy, more than 1% Fe or Ni addition is necessary in order to obtain a favorable volume fraction of strengthening phases by using RS technique. Kobayashi *et al.* [2] reported that the PM Al-2.2%Cu-1.5%Mg alloys with up to 7.0% Fe and 7.0% Ni additions were successfully dispersion strengthened by the fine dispersoids of $Al_9FeNi$ and age hardened by Al-Cu-Mg precipitates. The alloys were produced from coarse powders of 74–500 $\mu$m in diameter by the Conform method at ambient temperature [5]. On the other hand, Lim *et al.* [3] indicated that with addition of 4.0% Fe and 4.0% Ni, the age hardenability of PM 2024 alloy, which was extruded at 673 K from rapidly solidified flakes 40–50 $\mu$m in thickness, was decreased due to the formation of the insoluble compounds of Fe and/or Ni with Cu. According to our recent research [6], the microstructure of 2024Al-3.0mass%Fe-5.0mass%Ni powders strongly depended

TABLE I Chemical composition of the PM alloys (mass%)

| Alloy | Cu | Mg | Mn | Fe | Ni | Si | Zn | Cr/Ti | Al |
|---|---|---|---|---|---|---|---|---|---|
| 2024Al(2024) | 4.25 | 1.34 | 0.61 | tr | tr | 0.08 | 0.01 | tr | bal. |
| 2024Al-3Fe(3F0N) | 4.31 | 1.22 | 0.59 | 3.01 | 0.01 | 0.55 | tr | tr | bal. |
| 2024Al-3Fe-5Ni(3F5N) | 3.98 | 1.37 | 0.52 | 2.96 | 4.81 | 0.04 | 0.02 | tr | bal. |

on the powder diameter (cooling rate), and the amount of the insoluble compound $Al_7Cu_2Fe$ formed after extrusion was also influenced by the size range of starting powder and the extrusion temperature.

Therefore, the conclusion on IM alloy made by Wilson and Forsyth [4] should be checked again. Particularly, effects of alloying elements and processing condition, such as starting powder size and consolidation temperature, on the aging behavior should be carefully investigated in order to develop heat-treatable and age hardening alloys by using powder metallurgy method.

The present work is aimed to clear the age hardenability and the effects of powder size and extrusion temperature on the aging behavior of PM 2024Al-3mass%Fe-5mass%Ni(3F5N) alloy extrusions. The aging behavior of the 3F5N alloy extrusions is also compared with those of PM 2024Al (2024) and PM 2024 Al-3mass%Fe(3F0N) extrusions.

## 2. Experimental procedure

The chemical compositions of powder alloys used in this experiment are shown in Table I. The powder sieved with certain diameter range, ∼45 $\mu$m, 63–106 $\mu$m or ∼150 $\mu$m, were cold isostatically pressed and extruded to rectangular bar shape (section: 20 × 3.6 mm) in air at 623 K or at 723 K after holding for 1.8 ks at each extrusion temperature. The extrusion ratio was 10. After about one month at room temperature, the solution treatment of the extrusions was carried out at 748 K for 3.6 ks, followed by cold water quenching. After solution treatment, isothermal aging was performed at 373, 428, 448 or 473 K for over 360 ks in an air furnace. Hardness measurements during aging treatment were made by using a micro-Vickers hardness tester (weight: 200 g), and an average of at least six readings was taken for each measurement.

X-ray diffraction (XRD) analysis was carried out by Rigaku Rad1C, using a step scan mode, wave length Cu$K_{\alpha 1}$, slits: ds1.00° rs0.15 mm ss1.00°. The acceleration current and voltage were 20 mA and 40 kV, respectively. Lattice constants of the $\alpha$-Al matrix of the alloys were obtained by using the external standard method.

Thermal analysis of powders with different diameter was carried out by Differential Scanning Calorimetry (DSC) on Seiko DSC220C from room temperature to 773 K.

Transmission Electron Microscope (TEM) and Energy Dispersion of X-ray (EDX) specimens were prepared by cutting 3.0 mm discs along the extrusion direction and electropolishing. Thin foil samples were examined on JEM200 CX, operated at 200 kV.

## 3. Results and discussion

### 3.1. Age hardenability of PM 3F0N and 3F5N alloy extrusions

The Vickers hardness (*Hv*) vs. aging time curves of the 2024, 3F0N and 3F5N alloys extruded at 723 K from powders of 63–106 $\mu$m in diameter are shown in Fig. 1. With aging time, the *Hv* value of the 3F5N alloy gradually increased and reached to the peak value at each temperature. The maximum value for the 3F5N alloy was obtained at 428 K, which value was about 32 higher than that after solution treatment and quenched in water. Whereas, for the 3F0N and 2024 PM alloys, the maximum *Hv* values were also obtained at 428 K and were about 14 and 22.5 higher than that after quenching, respectively. The hardness increments ($\Delta Hv$) from the value after quenching to the maximum value for the 3F5N alloy are larger than those for the 2024 alloy at 428 and 448 K aging temperatures, respectively. However, the $\Delta Hv$ of the 3F0N alloy at each temperature is less than that of 2024 alloy. Therefore, the 3F5N alloy extruded at 723 K from powders of 63–106 $\mu$m in diameter is considered to have rather better age hardenability than the 2024 alloy extrusions. In contrast, the 3F0N alloy has poor age hardenability than the 2024 alloy.

Table II shows the results of precision analysis by XRD of $\alpha$-Al matrix lattice constants of the 2024, 3F0N and 3F5N alloy specimens cut from the same extrusions as used in Fig. 1. After quenching in water, $\alpha$-Al lattice constants of the 2024 and 3F5N extrusions were decreased by $2.22 \times 10^{-3}$ and $2.57 \times 10^{-3}$ Å, respectively, while that of the 3F0N extrusions was increased by $2.89 \times 10^{-3}$ Å.

At the solution temperature of 748 K, only Cu and Mg elements could be dissolved into the $\alpha$-Al matrix. Cu atom being smaller in diameter than Al atom and

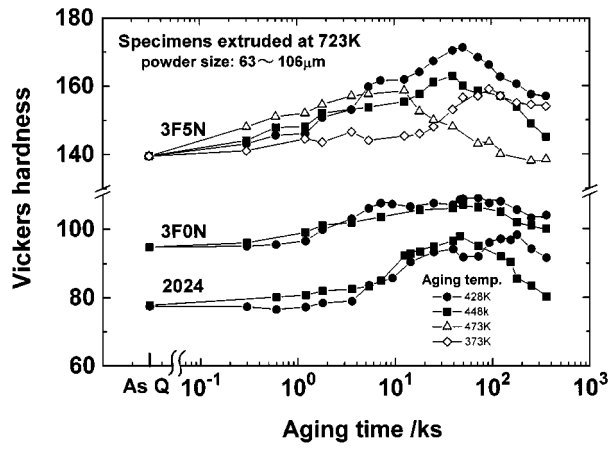


*Figure 1* Comparison of aging behavior during T6 treatment of PM 2024, 3F0N and 3F5N alloys extruded at 723 K from powders 63–106 $\mu$m in diameter, As Q--as quenched.

TABLE II Results of lattice constant $d$ (Å) of $\alpha$-Al matrix by XRD

| Alloy | Before solution treatment | After solution treatment | $\Delta d_{(A\text{-}B)}$ |
|---|---|---|---|
| 2024 | 4.05360 | 4.05138 | −0.00222 |
| 3F0N | 4.05607 | 4.05896 | +0.00289 |
| 3F5N | 4.05725 | 4.05468 | −0.00257 |

$\Delta d_{(A\text{-}B)}$: changes of $d$ values of $\alpha$-Al matrix during the solution treatment.

thus, it could decrease the Al lattice constant. On the other hand, Mg in solid solution would increase the Al lattice constant [7]. As no compound related to Mg element has been found in the 3F5N extrusions from the XRD results shown latter in Fig. 5 and also in 3F0N extrusions [8], all of Mg could be in solid solution in the three alloys after the solution treatment. Therefore, the change of Al lattice constant through the solution treatment could be mainly due to the amount of Cu dissolved into Al matrix. The result, which decrements of the lattice constants of $\alpha$-Al matrix of the 3F5N and 2024 alloys are about the same level, implies that the combined additions of Fe and Ni have a possibility of a fine dispersoid dispersion hardening without decreasing the age hardening capacity of an alloy with Cu by forming a nickel/iron rich phase containing little copper, such as $Al_9FeNi$ [4, 9].

On the other hand, the increase of lattice constant of the $\alpha$-Al matrix of the 3F0N alloy after 748 K solution treatment could be considered that the amount of solid solution Cu in the 3F0N alloy is much less than that in the 3F5N or 2024 alloy, resulting that the increment caused by Mg solid solution in the $\alpha$-Al matrix is larger than the decrement by Cu solid solution.

Figs 2a and b show the results of EDX analysis for the 3F0N and 3F5N alloys, respectively, extruded at

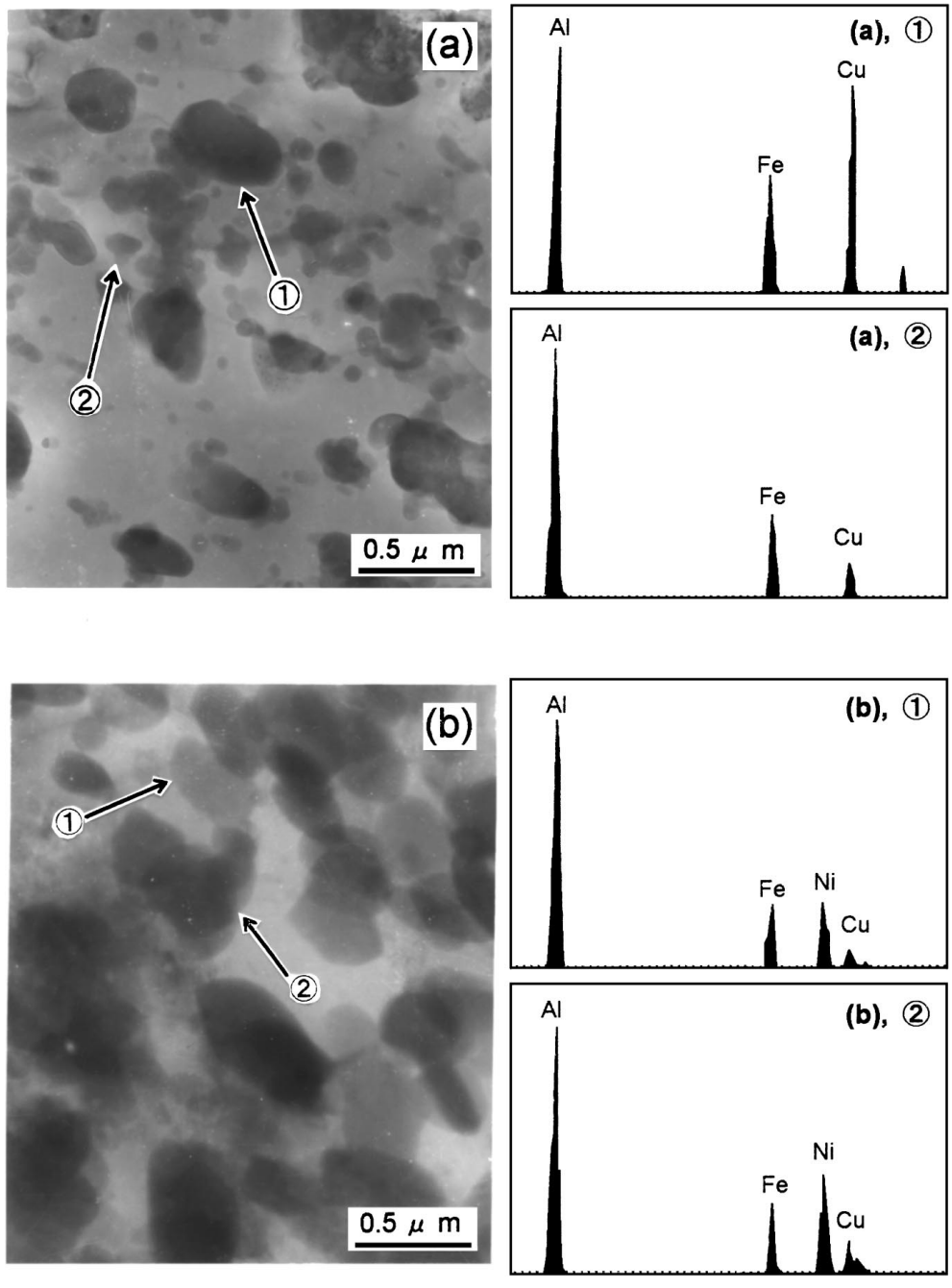


*Figure 2* EDX analyses for 3F0N (a), 3F5N (b) extrusions, ∼150 $\mu$m, $T_E$: 723 K, T6 treated.

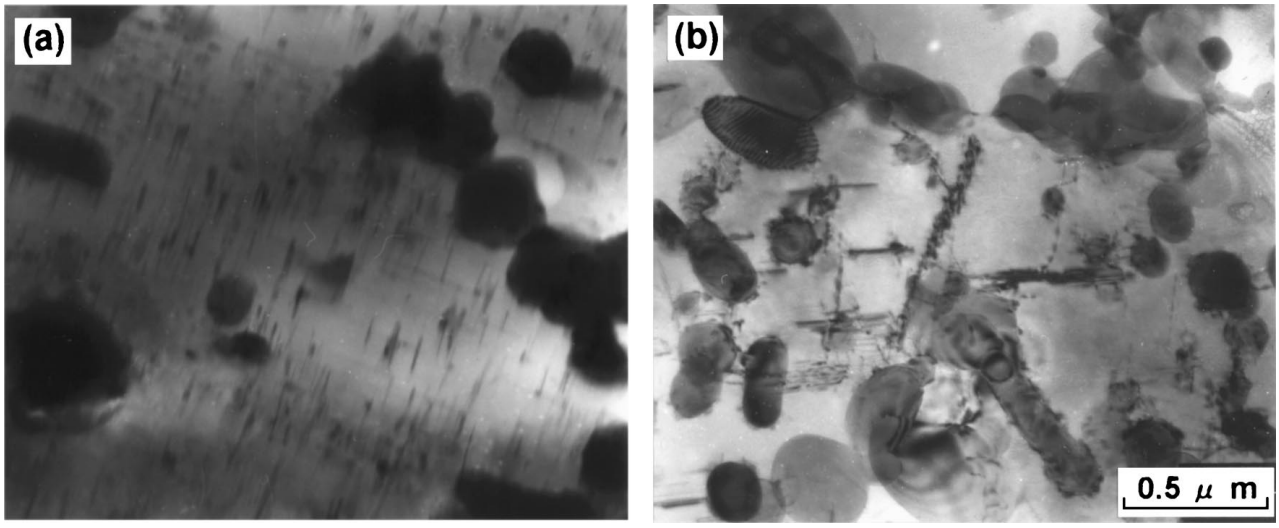


*Figure 3* TEM micrographs of 3F0N and 3F5N alloys extruded from powders 63–106 $\mu$m in diameter at 723 K with 748 K × 3.6 ks solution treated and aged at 473 K for 360 ks.

723 K followed by T6 treatment. From Fig. 2a, it can be seen that a large quantity of Cu was detected in the compounds, especially in the larger particles, which are considered to be $Al_7Cu_2Fe$ (see Fig. 2a) [8]. These Cu could not be dissolved into the matrix during solution treatment, and so resulting to a poor level of solid solution Cu in the $\alpha$-Al matrix in the 3F0N alloy. This result is well corresponding with that of lattice constant measurement. But in the 3F5N alloy, of which the main constituent particle is $Al_9FeNi$ phase [8], the amount of soluble Cu in compounds is little (see Fig. 2b). Therefore, in the 3F5N alloy, more Cu could be dissolved into $\alpha$-Al matrix as the solid solution state than in the 3F0N alloy.

Next, the difference of the precipitation behavior of (Al-Cu-Mg) phase was examined by TEM. It is known that, in Al-S phase pseudo-binary alloy as 2024Al alloy, G.P.B. (1) and (2) zones and S′ phase are formed with increasing aging time [10].

Figs 3a and b show TEM micrographs of the 3F0N and 3F5N alloys, respectively, extruded from powders 63–106 $\mu$m in diameter at 723 K, followed by 748 K × 3.6 ks solution treatment and over aging at 473 K for 360 ks. Coarse S′ phase was found after the over aging in both of the specimens. The contribution of the coarse precipitates of S′ phase to the age hardening in Al-Cu-Mg alloys is extremely smaller than that of fine G.P.B. zone precipitates [11]. However, a difference in the precipitate morphology of S′ phase was found between the 3F0N and 3F5N alloys. Compared Figs 3a and b, it could be seen that in the 3F0N alloy the rod-like S′ phases are precipitated relatively uniformly in the matrix (see Fig. 3a). However in the 3F5N alloy most of the S′ phases are seen to precipitate in lath morphology on or around the constituent particles (see Fig. 3b). It is reported that the concentration of (Cu+Mg) in the matrix affects the precipitation morphology of S′ phase in Al-Cu-Mg alloys, and with a higher (Cu+Mg) concentration lath formation becomes energetically favorable [12]. The result shown in Fig. 3 seemed to be well corresponding with that of Table II.

## 3.2. Effects of consolidation condition

The specimens of the 3F5N alloy extruded at 623 and 723 K, respectively, from the starting powders ∼45 $\mu$m in diameter were solution treated at 748 K and quenched in water, and then aged at 373, 428 and 448 K for 360 ks. The effect of extrusion temperature on age-hardening behavior of the 3F5N alloy is shown in Fig. 4. From Fig. 4, it is easily seen that Vickers hardness of the as-quenched 3F5N specimens extruded at 623 K is obviously higher than that extruded at 723 K. This difference in hardness of as-quenched state is mainly due to the finer constituent particles distributed in the 3F5N specimens extruded at lower temperature [6]. Fig. 4 also shows that the 3F5N specimens extruded at the lower temperature exhibited higher age hardenability than that extruded at 723 K at each aging temperature, although the peak aging time is not changed with extrusion temperature.

Based on Figs 1 and 4, the $\Delta Hv$ values of 3F5N alloy at each aging temperature are summarized in Table III. Effect of powder size on aging hardenability of the 3F5N alloy could be found in Table III. For the 3F5N alloy extruded at 723 K, $\Delta Hv$ was larger in the coarser starting powder size. For example, with increasing

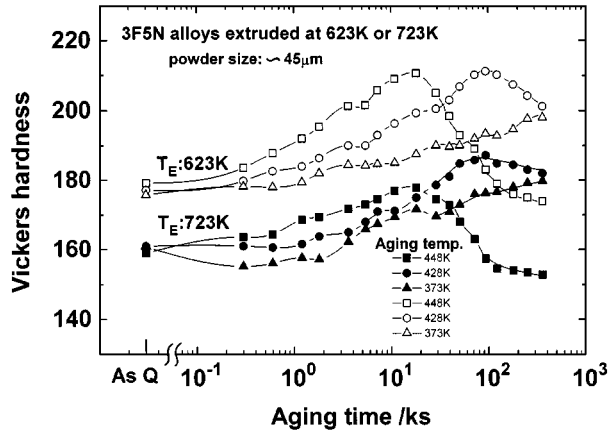


*Figure 4* Vickers hardness vs. aging time curves of 3F5N alloy extruded from powders ∼45 $\mu$m in diameter at 623 or 723 K, As Q--as quenched.

TABLE III *Hv* increment ($\Delta Hv$) of 3F5N alloy during the aging treatments

| Alloy | Powder diametre ($\mu$m) | Extrusion temperature (K) | Aging temperature (K) | $\Delta Hv$ ($Hv_{peak} - Hv_{quench}$) |
|---|---|---|---|---|
| 3F5N | ~45 $\mu$m | 623 | 428 | 33.8 |
| | | 623 | 448 | 31.5 |
| | | 723 | 428 | 26.0 |
| | | 723 | 448 | 17.5 |
| | 63–106 $\mu$m | 723 | 428 | 32.0 |
| | | 723 | 448 | 22.9 |

powder diameter from ~45 $\mu$m to 63–106 $\mu$m, the $\Delta Hv$ during 428 K aging was increased from about 26.0 to 32.0. However, this disadvantage in age hardening due to using finer powder can be overcome by lowering the extrusion temperature from 723 to 623 K.

Fig. 5 is the XRD patterns of the 3F5N specimens as extruded at 623 and 723 K from the powders less than 150 $\mu$m in diameter. The XRD pattern of the specimen extruded at 623 K followed by solution treatment at 748 K and quenching in water is also shown in Fig. 5 for the comparison. From Fig. 5, $Al_9FeNi$, $Al_7Cu_2Fe$, $Al_3Ni$ and $Al_3Fe$ compounds are found in 3F5N extrusion, and the intensity from $Al_7Cu_2Fe$ compound is the highest in the specimen extruded at 723 K. The solid solution treatment at 748 K for 1.8 ks did not increase the intensity of $Al_7Cu_2Fe$ of the specimen extruded at 623 K so much.

Fig. 6 is the results of DSC analysis for the 3F5N powders with six different ranges in diameter. The exothermic peak at about 523 K is common to the all samples, and is considered to be associated with the precipitation of S′ phase [13]. At over 673 K, the powders with diameter larger than ~45 $\mu$m show only a

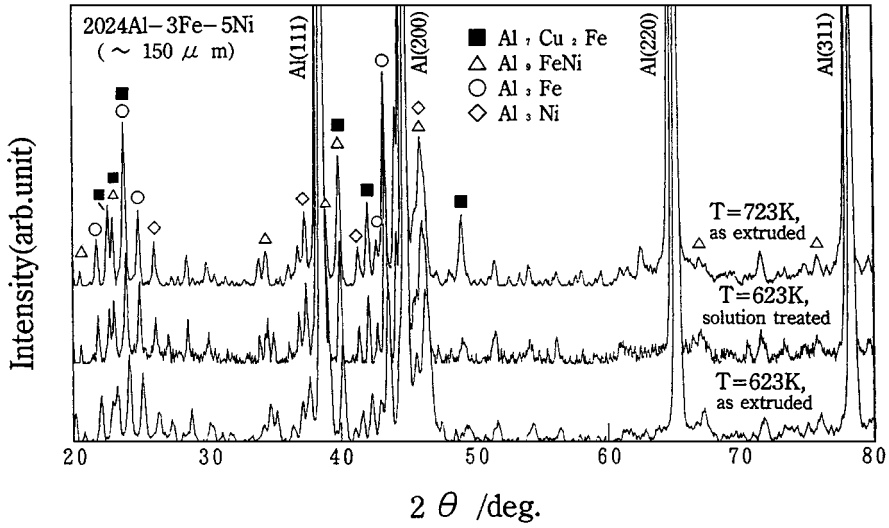


*Figure 5* XRD patterns for comparing $Al_7Cu_2Fe$ compound in specimens extruded from powders less than 150 $\mu$m in diameter at 723 and 623 K with or without solution treatment.

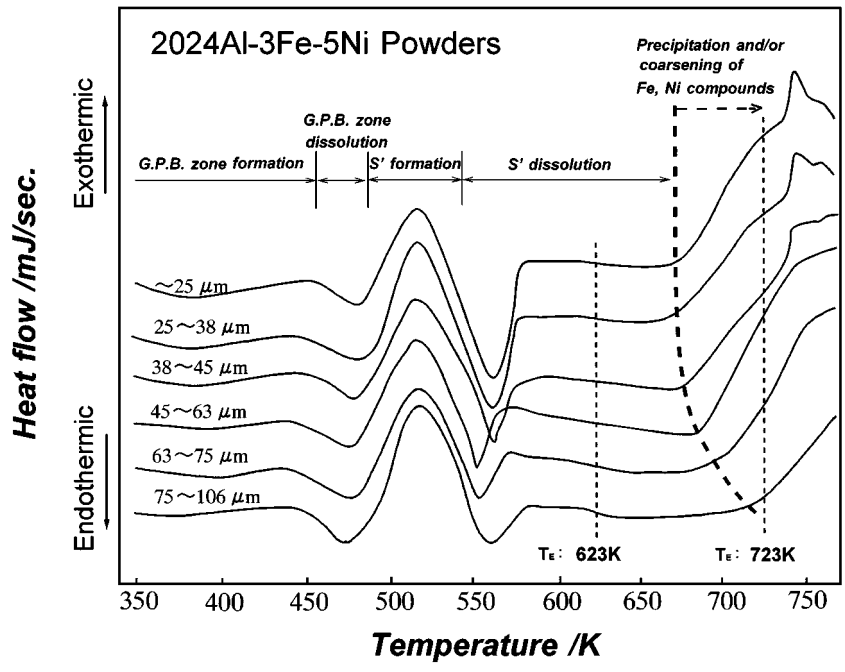


*Figure 6* DSC traces of six range of diameter powders of 3F5N alloy.

broad exothermic peak, but the smaller powders below ~45 $\mu$m in diameter exhibit an extra sharp peak in the broad peak. The extra sharp peak at about 740 K has been regarded to relate with the formation of $Al_7Cu_2Fe$ compound [6]. It is also clear to see that the beginning temperature of broad peak is increased from about 670 to 720 K with increasing the powder diameter from 25 to 106 $\mu$m, see the bold dash line in Fig. 6. This result is thought that with decreasing the powder size, the cooling rate was increased during the solidification of RS powders, resulting in increasing the supersaturation degree of alloying elements, such as Fe and Ni in the matrix [14]. Thus RS powders with finer diameter will, probably precipitate new compounds related the supersaturated alloying elements, and/or occur the coarsening of finer compound particles at a lower temperature.

From the above result, it is understood that at about 740 K, which is close to the higher extrusion temperature of 723 K, only in the powders less than 45 $\mu$m in diameter, $Al_7Cu_2Fe$ compounds are formed due to the combination of the supersaturated Fe, Ni elements with Cu in solid solution as well as Al. Thus, at higher extrusion temperature, which accelerates the diffusion of alloying element [15], the formation of more $Al_7Cu_2Fe$ compounds resulted in the finer powders. This result, on other word, presents that in the alloy extruded at lower temperature less insoluble compound $Al_7Cu_2Fe$ is formed, as shown in Fig. 5, and thus more Cu in solid solution resulted a higher age hardenability, as shown in Table III.

From Fig. 6, it is also known that at relatively low extrusion temperature (with the left region of the bold dash line, e.g. at 623 K) the effect of powder size on aging behaviors of the extrudates is little.

From the above analysis, it is easily found that extrusion temperature as well as powder diameter affect the aging hardenability of 3F5N alloy. In this experiment, relatively high aging hardenability could be obtained in the 3F5N alloy extruded at lower temperature and from the finer powders.

## 4. Conclusion

1. The extrusions of the 3F0N alloy, PM 2024Al with a 3 mass% Fe single addition, exhibited poor aging ability compared to the 2024 alloy. According to the results of EDX analysis and precision analysis of $\alpha$-Al matrix lattice constants of XRD, the amount of solid solution Cu in the 3F0N alloy matrix was found to decrease by forming of $Al_7Cu_2Fe$ compound during solidification. This resulted to lower the amount of Cu dissolved into $\alpha$-Al matrix during the solution treatment.

2. In the 3F5N alloy, PM 2024Al with a 3 mass% Fe and 5 mass% Ni combined addition, the amount of insoluble compound $Al_7Cu_2Fe$ during solidification was decreased by the formation of $Al_9FeNi$ phase, and thus, more Cu could be dissolved into the powder matrix.

3. However, during the extrusion at the higher temperature than about 740 K, the formation of the $Al_7Cu_2Fe$ compound was found in the finer 3F5N powders than about 45 $\mu$m in diameter. With decreasing the extrusion temperature, the aging ability as high as that of the PM2024Al could be obtained in the 3F5N alloy extruded even from the finer powders.


## Acknowledgements

The authors would like to thank Dr. Y. Nakamura of the materials science department of Toyama University for her Kindly helping in the XRD analysis.


## References


1. S. LIM, M. SUGAMATA and J. KANEKO, *J. Japan Inst. Light Metals* **37** (1987) 690.
2. Y. KOBAYASHI, M. YODA and Y. SUZUKI, *ibid.* **38** (1988) 338.
3. S. LIM, J. KANEKO and M. SUGAMATA, *ibid.* **41** (1991) 251.
4. R. N. WILSON and P. J. E. FORSYTH, *J. Inst. Metals* **94** (1966) 2332.
5. D. GREEN, *ibid.* **100** (1972) 295.
6. K. MATSUKI, S. XIANG, T. KIMOTO, M. TOKIZAWA, T. YOKOTE, J. KUSUI and K. FUJII, *Mater. Sci. Technol.* **13** (1997) 477.
7. U. SCHMIDT, R. UNGER and R. GERLOFF, *J. Mater. Sci.* **30** (1995) 3265.
8. K. MATSUKI, T. KIMOTO, S. XIANG, M. TOKIZAWA, T. YOKOTE, J. KUSUI and K. FUJII, *J. Japan Inst. Light Metals* **46** (1996) 189.
9. L. F. MONDOLFO, "Aluminum Alloys: Structure and Properties" (Butterworth, London, 1976).
10. J. M. SILCOCK, *J. Inst. Metals* **89** (1960–61) 203.
11. T. TAKAHASHI and T. SATO, *J. Japan Inst. Light Metals* **35** (1985) 41.
12. A. K. GUPTA, P. GAUNT and M. C. CHATURVED, *Phil. Mag.* **A55** (1987) 375.
13. W. J. BOETTINGER, L. BENDERSKY and J. G. EARLY, *Met. Trans. A* **17A** (1986) 781.
14. J. M. PAPAZIAN, *ibid.* **19A** (1988) 2945.
15. S. FUJIKAWA, *J. Japan Inst. Light Metals* **46** (1996) 202.



*Received 21 May 1997*
*and accepted 9 November 1998*